

## Cardioprotective Effects of Dapagliflozin Against Radiotherapy Induced Cardiac Damage

### ABSTRACT

**Background:** With the increasing incidence of cancer among the adult population, radiotherapy (RT) is frequently used as a critical component in the treatment of various cancer types. Due to the nature of ionizing radiation, damage usually occurs within the tissues in anatomical neighborhood with the primary tumor localization. Dapagliflozin (DAPA), originally developed as an oral anti-diabetic medication, has been shown to have potent cardioprotective effects in the DAPA-HF trial. The cardioprotective effects of DAPA against RT induced cardiac cellular damage were investigated in this study.

**Methods:** A total of 40 male Wistar albino rats were obtained and were subjected to a 10-day pretreatment period to accommodate laboratory settings. Afterwards, the rats were divided into 4 groups consisting of 10 each (control = 10, DAPA = 10, RT = 10, RT + DAPA = 10). Meanwhile, the RT and RT + DAPA groups received a single dose of 20 Gray (Gy) x-ray to 4 × 4 cm area at 0.60 Gy/min, and DAPA and RT + DAPA groups were gavaged daily with 10 mg/kg DAPA. In the second week of the study, rats were examined by echocardiography and electrocardiogram. Furthermore, histopathological method was used to evaluate the level of cardiotoxicity.

**Results:** The ejection fraction value decreased by 17.3% lower in the DAPA + RT group compared with the RT group ( $P < .001$ ). In addition, corrected QT interval prolongation and QRS widening were 11.5% and 17.4% higher in the RT group compared with the DAPA + RT group, respectively ( $P < .001$  for both values). While sarcomyolysis, inflammatory cell infiltration, and necrotic changes were found to be severe in the RT group, the DAPA + RT group had 68% less sarcomyolysis, 64% less inflammatory cell infiltration, and 55% less necrosis ( $P < .001$  for all values).

**Conclusions:** The protective effects of DAPA against left ventricular remodeling and dysfunction in RT-induced cardiomyopathy model were observed in this study.

**Keywords:** Cardiomyopathy, left ventricular dysfunction, radiotherapy, SGLT-2 inhibitors

### INTRODUCTION

With increasing incidence of cancer among the adult population, radiotherapy (RT) is frequently used as a critical component in the treatment of various cancer types. Due to the nature of ionizing radiation, damage usually occurs within the tissues in anatomical neighborhood with the primary tumor localization. Thus, it is common for patients receiving RT for tumors located in the thorax to develop concomitant cardiac damage.<sup>1,2</sup> The proportion of cardiac damage induced is affected by endogenous and exogenous factors. Endogenous factors include susceptibility to irreversible cardiomyocyte injury due to systemic and cellular-level factors, and exogenous factors mainly consist of the cumulative amount of RT applied. Due to these variables, clinical end-results of cardiac damage vary from being asymptomatic to fully developed heart failure (HF).<sup>3</sup> This wide spectrum of cardiac toxicity is named radiation-induced heart disease (RIHD) and encompasses cardiomyopathy, pericarditis, coronary artery disease, and conduction system disorders.

Dapagliflozin (DAPA), originally developed as an oral anti-diabetic medication classified as a sodium-glucose cotransporter-2 (SGLT-2) inhibitor, has shown potent cardioprotective effects in the DAPA-HF trial.<sup>4</sup> Due to these effects, DAPA

### ORIGINAL INVESTIGATION

Mehmet Hakan Uzun<sup>1</sup> 

Aziz Erden<sup>2</sup> 

Sebahat Ulusan<sup>3</sup> 

Emine Elif Özkan<sup>4</sup> 

Alper Özseven<sup>4</sup> 

Kanat Güllü<sup>5</sup> 

Adnan Şahin<sup>6</sup> 

Selim Süleyman Sert<sup>6</sup> 

Kadir Şeker<sup>6</sup> 

Hüseyin Emre Cebeci<sup>6</sup> 

Muhammet Ali Ekiz<sup>6</sup> 

Seda Aydoğdu<sup>2</sup> 

Adnan Karabrahimoğlu<sup>7</sup> 

Mevlüt Serdar Kuyumcu<sup>6</sup> 

<sup>1</sup>Department of Cardiology, Republic of Türkiye Ministry of Health, Kütahya City Hospital, Kütahya, Türkiye

<sup>2</sup>Süleyman Demirel University, Faculty of Medicine, Isparta, Türkiye

<sup>3</sup>Republic of Türkiye Ministry of Health, Ankara, Türkiye

<sup>4</sup>Department of Radiation Oncology, Faculty of Medicine, Süleyman Demirel University, Isparta, Türkiye

<sup>5</sup>Department of Histology and Embryology, Faculty of Medicine, Süleyman Demirel University, Isparta, Türkiye

<sup>6</sup>Department of Cardiology, Faculty of Medicine, Süleyman Demirel University, Isparta, Türkiye

<sup>7</sup>Department of Biostatistics and Medical Informatics, Faculty of Medicine, Süleyman Demirel University, Isparta, Türkiye

#### Corresponding author:

Mehmet Hakan Uzun

✉ mdmehmetuzun@gmail.com

**Received:** September 8, 2024

**Accepted:** January 20, 2025

**Available Online Date:** March 4, 2025

**Cite this article as:** Uzun MH, Erden A, Ulusan S, et al. Cardioprotective effects of dapagliflozin against radiotherapy induced cardiac damage. *Anatol J Cardiol.* 2025;XX(X):1-8.

DOI:10.14744/AnatolJCardiol.2025.4818



Copyright@Author(s) - Available online at anatoljcardiol.com.  
Content of this journal is licensed under a Creative Commons Attribution-NonCommercial 4.0 International License.

has been added as part of the standard treatment of HF in all current guidelines. The molecular mechanisms of these cardioprotective effects are mainly attributed to changes in intracellular  $Ca^{2+}$  handling and antioxidant effects, but no definite mechanism has been shown to this day.<sup>5,6</sup> Various experimental trials based on this effect have shown DAPA has cardioprotective effects against various cardiotoxic factors.<sup>7-9</sup> In the best of current knowledge, no research has been published on the cardioprotective effects of SGLT-2 inhibitors against the cardiotoxic effects of RT. In addition, no exact molecular mechanisms of the cardioprotective effects of SGLT-2 inhibitors have been discovered yet.

In this study, the cardioprotective effects of DAPA against RT induced cardiac cellular damage were investigated.

## METHODS

Forty male Wistar albino rats were used in the study. Throughout the experiment, all animals were housed in the same facility, which was temperature-controlled (22-24°C) and maintained on a 12-hour light/dark cycle. The animals were fed an ad libitum diet during the study. The experiment was conducted in accordance with the Universal Declaration of Animal Rights, and the study received Ethical Approval from the Animal Experiments Local Ethics Committee.

After a 10-day pretreatment period, a total of 40 male Wistar albino rats were randomly divided into 4 groups consisting of 10 each (control = 10, DAPA = 10, RT = 10, RT + DAPA = 10). Moreover, all rats were assigned and selected randomly for a study in the animal research center. Male mice were preferred in the first stage of cardio-oncology studies because they are less affected by hormonal changes. Meanwhile, RT and RT + DAPA groups received a single dose of 20 Gray (Gy) x-ray to 4 × 4 cm area at 0.60 Gy/min, and DAPA and RT + DAPA groups, starting from 1 day after RT in order to minimize drug interactions between DAPA and anesthetics, were daily gavaged with 10 mg/kg DAPA for 2 weeks. Radiotherapy and DAPA doses were planned in accordance with other experimental designs in the current literature. In the second week of the study, rats were examined by echocardiography (ECHO) and electrocardiogram (ECG). Furthermore, histopathological method was used to evaluate the level of cardiotoxicity

## HIGHLIGHTS

- It was found that the radiotherapy (RT) group experienced a 17.3% more decrease in ejection fraction (EF) compared with the RT + Dapagliflozin (DAPA) group. Even though both groups' EF were >50%, statistically significant decrease was shown in the RT group.
- Histological evaluation of cardiac tissues showed that the RT + DAPA group had significantly less inflammatory response, compared with the RT group.
- The QRS, PR, and QTc values deteriorated significantly less in the RT + DAPA group, indicating potent cardioprotective effects of DAPA on the cardiac conduction system.

(Figure 1). No animal losses were observed during the pre-treatment and the treatment periods.

The sample size was calculated according to a crude method for the sample size calculation of animal studies. In this method, a value "E" is measured for ANOVA, and it should lie between 10 and 20. For the formula  $E = \text{total number of animals} - \text{total number of groups}$ , minimum sample size was calculated as  $E = (10 \times 4) - 4 = 36$ , and was considered as adequate.<sup>10</sup>

## Electrocardiogram

The electrocardiograph machine (Fukuda Denshi Co. Ltd., Tokyo, Japan) was employed to conduct ECGs. Electrodes were positioned on the right wrist, sternum, right ankle, and left ankle of the anesthetized rats. Electrocardiograms were carried out both at baseline and at the conclusion of 2 weeks.

## Echocardiographic Imaging

The Philips Lumify ECHO system with the standard adult type S4-2 model transducer (Koninklijke Philips N.V., Amsterdam, Netherlands) was used to obtain images from all animals at baseline (n = 40). All images were obtained with the standard adult ECHO preset, using the zoom-in function of the application with a standard proportion of 8× zoom in all images. All animals were evaluated before receiving the first dose of RT and DAPA. Two weeks after the start of the experiment, the heart functions of all animals were assessed using 2-dimensional ECHO.

## Histopathological Examination

Animal heart tissues were preserved using a 10% buffered formaldehyde solution. Prior to processing the tissues, they underwent an overnight wash with running tap water, were dehydrated gradually in ethanol, treated with xylene for clearing, and finally embedded in paraffin. Thin sections measuring 4-5 μm were then obtained from the paraffin blocks and subjected to staining with hematoxylin and eosin. Evaluation of the tissue samples was carried out through histopathological examination using a light microscope. A modified semiquantitative scoring system was applied based on the identified findings: (0) for no findings, (+1) for a low level of findings, (+2) for moderate findings, and (+3) for severe findings. A modified semiquantitative scoring system was applied according to the determined findings. Findings were evaluated in terms of sarcomyolysis, fragmented fibrils and necrotic changes and were classified as (0) no pathological findings, (+1) low-level damage (or can be written as pathological) findings, (+2) moderate damage, and (+3) severe damage.

## Statistical Analysis

The statistical analyses were performed using SPSS 27.0 (IBM Inc., Armonk, NY, USA) software. The descriptive statistics were presented as mean ± SD for numerical variables and frequency (percentage) for categorical variables. The Shapiro-Wilk test was used to determine the normality of the continuous measurements. Since the distributions were normal, comparison analyses were performed using parametric methods. The measurements were conducted in 4 study groups and at 2 time periods (baseline and after 2

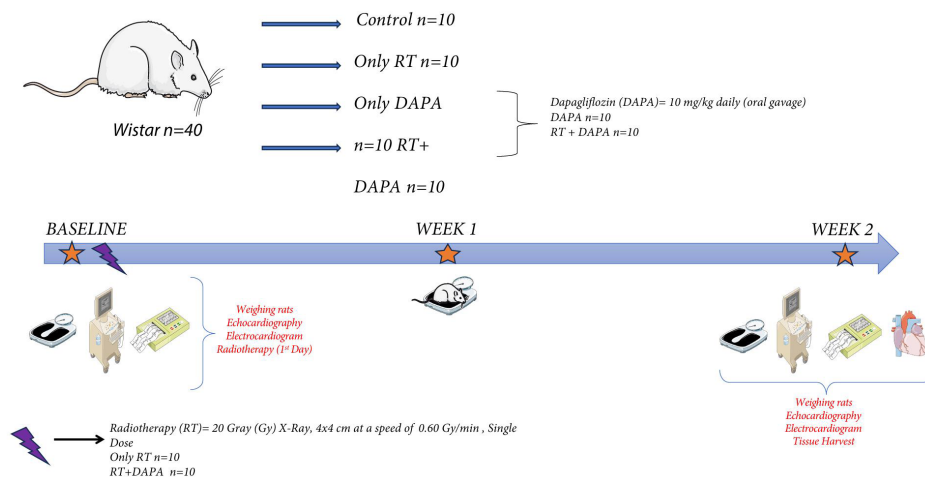


**Figure 1. Study protocol.**

weeks). Therefore, the comparison between the groups and the periods was performed using 2-way repeated measure ANOVA (mixed type ANOVA) with TUKEY HSD post-hoc test for significant results, and significant pairs were indicated by the same superscript letters. The homogeneity of variances was assessed through the mean-based Levene test and Box's M test. The Kruskal–Wallis test was employed to compare the histopathological results between the study groups with K–W critical difference post-hoc test. Interobserver agreement for ECG and ECHO measurements was determined using the intraclass correlation coefficient (ICC), while interobserver agreement of histopathological evaluation was assessed by Kendall's Tau-b test. A  $P < .05$  value was considered a statistically significant result with a type-1 error of 5% in all analyses.

## RESULTS

The cardiac measurements and ECG results of the animals were compared before and after treatment (Table 1). Ejection fraction (EF) values did not differ between the study groups before treatment but showed a significant difference after treatment ( $P < .001$ ). Ejection fraction values decreased significantly in the RT group compared to the other groups ( $61.50 \pm 8.72$  vs.  $79.80 \pm 2.20$ ,  $79.90 \pm 2.38$ , and  $73.20 \pm 3.29$ , respectively). While EF value decreased in both groups, the EF value decrease was statistically lower in the post-treatment period in the RT + DAPA group than RT group ( $P < .001$ ). Fractional shortening (FS) before and after treatment also changed significantly between the groups ( $39.70 \pm 5.79$  vs.  $47.20 \pm 3.52$ ,  $48.00 \pm 4.24$ , and  $42.40 \pm 5.56$ , respectively). Fractional shortening values deteriorated more in the post-treatment period in the RT group compared with the RT + DAPA group ( $P < .001$ ). No statistically significant changes were observed in EF and FS values in the control and DAPA groups. The interobserver agreement for ECG and ECHO measurements was significantly high, and ICC values were calculated between 0.938 and 0.991 and 0.912 and 0.977, respectively.

The weights of the rats were assessed at 2 different time points. In general, a notable increase in the weight loss rate was observed over the course of the study. Basal weight was

lower in the DAPA group but was similar within the other groups. Inter-group weight loss was highest in the RT + DAPA group after treatment ( $P < .001$ ). Statistically significant weight loss was also observed between the control and DAPA groups ( $P < .001$ ).

Left ventricular end-systolic dimension (LVESD) and left ventricular end-diastolic dimension (LVEDD) measurement deterioration was statistically significantly lower in the RT + DAPA group than the RT group ( $P < .001$ ). Heart rate values were significantly higher in the post-treatment period in both RT and RT + DAPA groups ( $P < .001$ ), with the RT + DAPA group showing less increase in HR than the RT group ( $P < .001$ ). The PR, QRS, and QTc values were measured, and deterioration was found to be statistically higher in the RT group than in the RT + DAPA group ( $P < .001$ ) (Figure 2). No statistically significant changes occurred in the control and DAPA groups' HR, PR, QRS, and QTc values.

In histopathological evaluation, findings were classified as no, low, moderate, and severe. The control group was evaluated in terms of sarcomyolysis, fragmented fibrils and necrotic changes, and no findings were found. Likewise, it was stated as no pathological findings in the DAPA group. Low levels of sarcomyolysis and fragmented fibrils were observed in the RT + DAPA group. Necrotic changes were classified as moderate. In the RT group, severe sarcomyolysis, severe fragmented fibrils, and severe necrotic changes were detected. Intracellular inflammatory infiltration evaluation was found to be significantly higher in the RT group ( $P < .001$ ). The general infiltration value of the group was found to be "severe." Similarly, sarcomyolysis and necrotic changes were significantly higher and "severe" in the RT group ( $P < .001$ ) (Figures 3-6). While no positive results were found in the control and DAPA groups, low and moderate results were obtained in the RT + DAPA group (Table 1).

## DISCUSSION

Radiation-induced cardiac toxicity arises from increased oxidative stress (OS), endothelial dysfunction, damage to mitochondria and the endoplasmic reticulum (ER), and increased inflammation. Endothelial dysfunction disrupts

**Table 1. Cardiac, Histochemical, and ECG Measurements of Animals According to Study Groups**

	Control	DAPA	RT	RT + DAPA	<i>P</i> <sub>groups</sub>	<i>P</i> <sub>measures</sub>	<i>P</i> <sub>groups*measure</sub>
	Mean ± SD	Mean ± SD	Mean ± SD	Mean ± SD			
First measured weight (g)	323.20 ± 58.66	310.00 ± 55.70	325.50 ± 15.09	325.10 ± 25.34			
Last measured weight (g)	320.80 ± 57.91 <sup>a</sup>	281.60 ± 47.25	308.70 ± 28.18 <sup>b</sup>	257.00 ± 18.62 <sup>a,b</sup>	.515	<.001*	.024*
EF, baseline (%)	79.80 ± 2.86	79.20 ± 1.87	78.10 ± 2.60	79.00 ± 2.31	–		
EF, week 2 (%)	79.80 ± 2.20 <sup>a</sup>	79.90 ± 2.38 <sup>b</sup>	61.50 ± 8.72 <sup>a,b,c</sup>	73.20 ± 3.29 <sup>c</sup>	<.001	<.001	<.001
FS, baseline (%)	47.40 ± 3.24	47.40 ± 4.14	48.70 ± 3.92	48.80 ± 4.44			
FS, week 2 (%)	47.20 ± 3.52 <sup>a</sup>	48.00 ± 4.24 <sup>b</sup>	39.70 ± 5.79 <sup>a,b,c</sup>	42.40 ± 5.56 <sup>c</sup>	.200	<.001*	<.001*
End-diastolic volume, baseline (mL)	277.70 ± 10.98	272.10 ± 17.37	274.50 ± 11.19	277.20 ± 16.92			
End-diastolic volume, week 2 (mL)	276.40 ± 9.97 <sup>a</sup>	268.20 ± 17.22 <sup>b</sup>	310.30 ± 37.53 <sup>a,b,c</sup>	282.80 ± 12.99 <sup>c</sup>	.033*	<.001*	<.001*
End-systolic volume, baseline (mL)	57.80 ± 9.90	64.60 ± 8.66	56.40 ± 7.40	63.90 ± 9.94			
End-systolic volume, week 2 (mL)	56.70 ± 7.65 <sup>a,b,c</sup>	64.50 ± 10.02 <sup>a</sup>	68.10 ± 7.98 <sup>b</sup>	69.40 ± 10.49 <sup>c</sup>	.110	<.001*	<.001*
Heart rate, baseline (BPM)	321.70 ± 24.76	342.50 ± 29.69	345.10 ± 14.69	341.90 ± 25.24			
Heart rate, week 2 (BPM)	327.80 ± 24.44 <sup>a</sup>	345.70 ± 32.94 <sup>b</sup>	387.60 ± 33.12 <sup>a,b</sup>	354.60 ± 20.86	.006*	<.001*	<.001*
QTc, baseline (msn)	172.00 ± 18.38	168.00 ± 14.16	169.60 ± 12.29	173.90 ± 16.76			
QTc, week 2 (msn)	172.40 ± 18.7 <sup>a</sup>	168.60 ± 14.85 <sup>b</sup>	201.90 ± 25.63 <sup>a,b,c</sup>	179.10 ± 16.58 <sup>c</sup>	.135	<.001*	<.001*
PR, baseline (msn)	42.70 ± 6.53	41.20 ± 4.54	42.60 ± 4.01	44.10 ± 6.26			
PR, week 2 (msn)	43.00 ± 5.89 <sup>a</sup>	41.20 ± 4.94 <sup>b</sup>	58.40 ± 9.89 <sup>a,b,c</sup>	48.20 ± 7.96 <sup>c</sup>	.005*	<.001*	<.001*
QRS, baseline (msn)	14.30 ± 2.21	14.20 ± 1.81	14.60 ± 2.95	14.80 ± 2.04			
QRS, week 2 (msn)	14.50 ± 2.17 <sup>a</sup>	14.50 ± 1.90 <sup>b</sup>	19.90 ± 4.77 <sup>a,b,c</sup>	16.70 ± 2.31 <sup>c</sup>	.019*	.001*	.001*
Inflammatory cell infiltration	0.2 ± 0.4 (0: 0-1)	0.2 ± 0.4 (0: 0-1)	2.8 ± 0.4 <sup>+</sup> (3: 1-3)	1.0 ± 0.8 (0: 0-1)	.001**		
Sarcomyolysis	0.0 ± 0.0 (0: 0-0)	0.0 ± 0.0 (0: 0-1)	3.2 ± 0.4 <sup>+</sup> (3: 1-3)	1.0 ± 0.8 (0: 0-1)	<.001**		
Necrotic changes	0.0 ± 0.0 (0: 0-0)	0.0 ± 0.0 (0: 0-0)	3.0 ± 0.0 <sup>+</sup> (3: 3-3)	1.4 ± 0.8 (0: 0-2)	<.001**		

Data are given as mean ± standard deviation (SD), median (min-max) where necessary.

BPM, beats per minute; EF, ejection fraction; FS, fractional shortening; mL, milliliters; msn, milliseconds; QTc, corrected QT interval.

\*Significant at the 0.05 level according to 2-way repeated measure ANOVA.

<sup>a,b,c</sup>Same superscript letters denote the significant pairwise comparisons according to Tukey HSD post-hoc test.

\*\*Significant at the 0.05 level according to Kruskal–Wallis test.

<sup>+</sup>Sign indicates the significant difference between the groups.

the myocardial blood supply, resulting in cellular ischemia.<sup>11</sup> Radiation exposure also affects coagulation functions and platelet activity, increasing the deposition and release of von Willebrand factor (vWF) in the endothelial cells.<sup>12</sup> The changes in vWF expression ultimately result in increased platelet adhesion and thrombosis in capillaries, further increasing cellular ischemia.

Radiation induced cellular damage following radiation exposure is primarily caused by the generation of reactive oxygen species (ROS) due to the radiolysis of water, which serves as a significant source of normal tissue damage after ionizing radiation. Reactive oxygen species can directly damage intracellular macromolecular structures and alter the expression of various proteomes in the cytoplasm, leading to the activation of pro-inflammatory factors associated with ROS.<sup>13</sup> The NF-κB plays a crucial role in regulating DNA transcription and protein complexes involved in various cellular stress responses, potentially acting as a key regulator linking OS and inflammation. Reactive oxygen species functions as a second messenger to activate NF-κB, leading to the production of inflammatory cytokines. As a result, proinflammatory cytokines and chemokines are thought to be closely associated with the onset of OS, while the

inflammation intensified by OS further drives disease progression.<sup>14</sup> Excessive ROS production by mitochondria in human cells has been observed immediately following irradiation.<sup>15</sup> Mitochondrial dysfunction is closely linked to the occurrence of ER stress. After cardiac myocytes are irradiated, the ER releases calcium ions from its calcium stores into the cytoplasm. This process results in mitochondrial calcium overload, leading to membrane swelling and the release of apoptotic factors from the mitochondria, thus triggering apoptosis. While SGLT2 inhibitors have been shown to mitigate oxidative stress through reductions in reactive oxygen species (ROS) production and improvements in mitochondrial function, the exact molecular mechanisms underlying these protective effects remain incompletely understood, highlighting a critical gap in current evidence that warrants further investigation.

In order to avoid animal losses before completion of the protocol due to RT-induced acute cardiotoxicity, the RT dose was determined based on numerous rat model experiments on cardiac RT in the literature.<sup>16-18</sup> Radiation-induced heart disease development increases significantly after 20 Gy of RT application.<sup>19,20</sup> In current literature, acute inflammatory changes in histopathology,

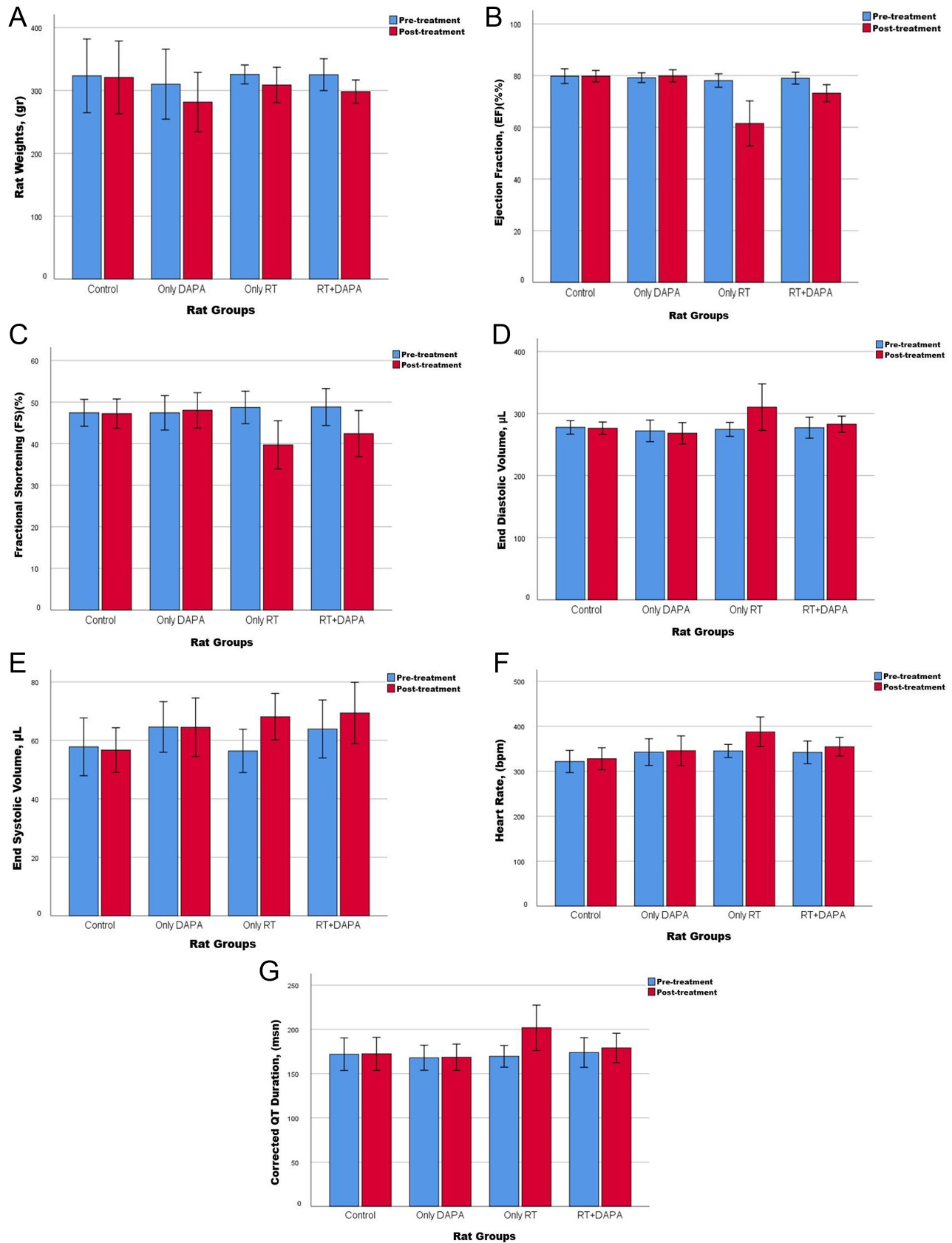
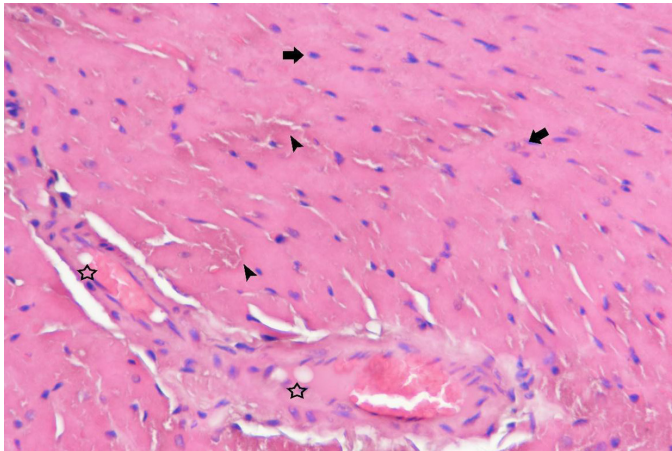
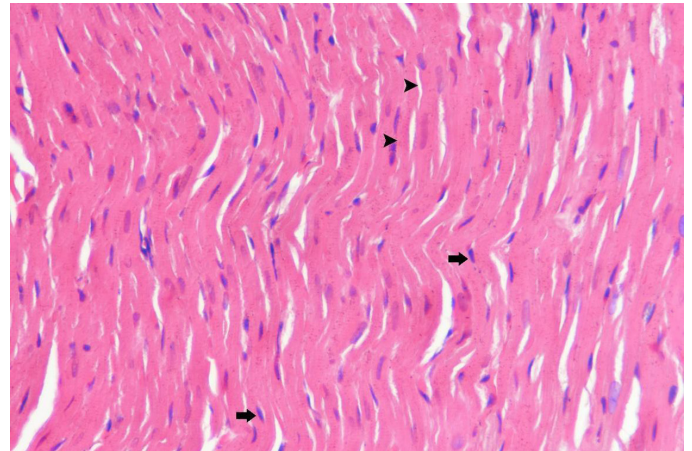


Figure 2. (A) Basal and week 2 weight charts. (B) Basal and week 2 ejection fraction charts. (C) Basal and week 2 fractional shortening charts. (D) Basal and week 2 left ventricular end-diastolic dimension charts. (E) Basal and week 2 left ventricular end-systolic dimension charts. (F) Basal and week 2 heart rate charts. (G) Basal and week 2 QTc duration charts.





**Figure 3. RT group. Section of the myocardial layer. Dense fragmented fibril accumulation (arrowhead), necrotic changes in the nuclei of muscle cells (thick arrow), locally vacuolized areas (asterisk), and intense sarcomyolysis were observed. Additionally, vascular structures with impaired vessel wall integrity and intense sarcomyolysis were observed (HE ×40) ( $P < .001$ ).**



**Figure 5. DAPA group. Section of the myocardial layer. No fibrin deposition was observed, normal nuclear structures were observed, and sarcomyolysis was not observed (HE ×40) ( $P < .001$ ).**

development of left ventricular (LV) diastolic dysfunction, and increases in cardiac dimensions are detectable 1 week after RT application.<sup>21,22</sup> Radiotherapy-induced chronic fibrosis development becomes apparent after 12 weeks in the rat models.<sup>23</sup>

In this study, the RT group that received DAPA showed less deterioration in parameters such as QRS duration, QT duration, and basal heart rate—key predictors of arrhythmogenic events—compared to the group that did not receive DAPA. In the DAPA-HF study, the group receiving DAPA experienced a significantly lower incidence of severe ventricular arrhythmias (5.9% vs. 7.4%) and a 21% relative risk reduction compared to the placebo group.<sup>24</sup> Another meta-analysis also reported a significant reduction in the incidence

of atrial arrhythmias among those receiving SGLT-2 inhibitor therapy.<sup>25</sup>

Although decreases in EF and FS values were statistically significantly more in the RT group compared with the RT + DAPA group, mean EF values were above 50% in both groups. LVEDD and LVESD values were increased in both groups, but were found to be statistically significantly higher in the RT group. The most common echocardiographic findings in RIHD include regional wall motion abnormalities, mild LV global hypokinesia, and impaired diastolic functions, and our findings were consistent with the current literature data.<sup>26,27</sup> Progression of fibrosis eventually results in the development of systolic dysfunction.<sup>28</sup> This process takes time, which may take up to 10-15 years in humans who receive RT, and the degree of EF deterioration as well as its effect on the prognosis is not well established in RIHD.<sup>27</sup> Even though the degree of acute inflammatory response correlates with the development of chronic changes, this process is multifactorial and developing new methods for screening the patients

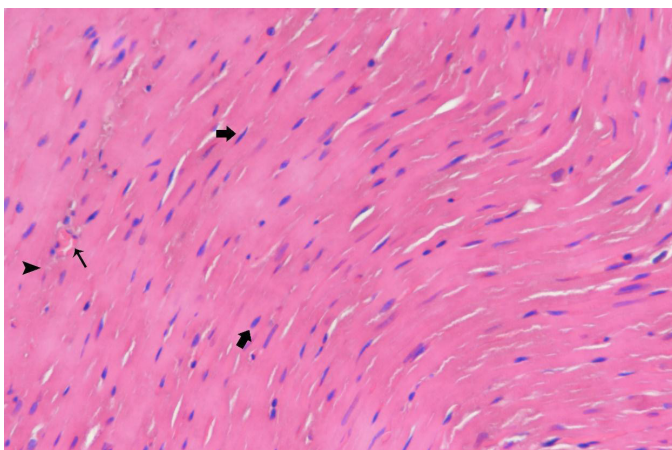


**Figure 4. RT + DAPA group. Section of the myocardial layer. Compared to the RT group, less fibrin deposition (arrowhead), less necrotic changes (thick arrow), intact capillaries (thin arrow), and properly aligned cardiac muscle fibers were observed (HE ×40) ( $P < .001$ ).**

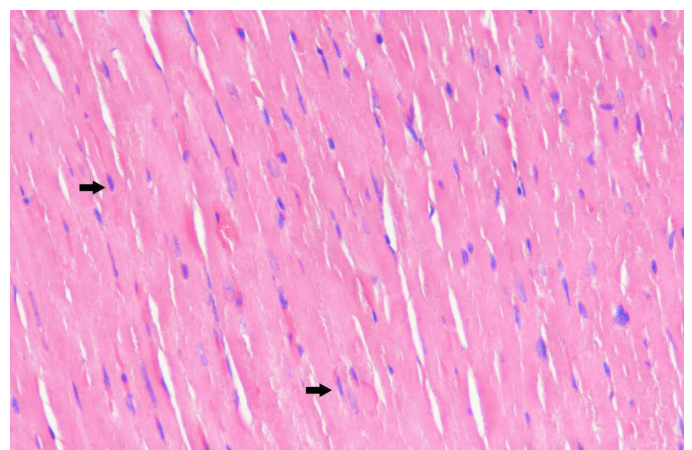


**Figure 6. Control group. Cardiac muscle fibers, nuclei (arrow), and fiber alignment were observed in near-normal histology (HE ×40) ( $P < .001$ ).**

to detect which are under increased risk of developing RIHD continues to this day.<sup>29</sup> Due to the cardiac anti-fibrotic effects of SGLT-2 inhibitors shown in HF patients, we believe more research is required in this field to investigate potential therapies in preventing the development of RIHD.

Finally, the study has shown that the histopathologic inflammatory response and consequent development of myocardial fibrosis are greatly reduced in the group that received DAPA with RT. However, due to the lack of sufficient experimental data specific to RT, further clinical studies are needed. Validating the current findings in this context will be important in assessing the applicability of DAPA as a cardioprotective agent against radiotherapy-induced cardiomyopathy. Further research in this area is needed in order to evaluate the mechanisms that contribute to the anti-oxidative and anti-inflammatory effects of DAPA against RT.

### Study Limitations

Due to the inability to examine rat models for ventricular strain patterns and diastolic dysfunction parameters, the development of LV diastolic dysfunction, the changes in ventricular strain patterns in RT groups, and the possible cardioprotective effects of DAPA against RT-induced diastolic dysfunction could not be evaluated. In addition, healthy rats without cancer were used in the study. Further investigations are required to enhance the understanding of the cardioprotective effects of DAPA in humans receiving RT for malignancies.

### CONCLUSIONS

In this study, the protective effects of DAPA against LV remodeling and dysfunction in RT-induced cardiomyopathy model were observed. Additionally, treatment with DAPA was found to mitigate the deterioration of RT-induced arrhythmia parameters. Weight loss occurs in both RT and DAPA therapies; therefore, cardioprotective treatment with DAPA in RT may result in increased weight loss, which may deteriorate the nutritional status of already fragile cancer patients. Future investigations should prioritize exploring the cardiac function protective characteristics of DAPA in the context of RT-induced cardiotoxicity in large animal models and cancer patients.

**Ethics Committee Approval:** The experiment was conducted in accordance with the Universal Declaration of Animal Rights, and the study received ethical approval from the Süleyman Demirel University Animal Experiments Local Ethics Committee with number 04/271 on March 28, 2024.

**Informed Consent:** Due to the design of this study as an animal experiment, informed consent wasn't obtained.

**Peer-review:** Externally peer-reviewed.

**Author Contributions:** Concept – M.H.U., M.S.K.; Design – M.H.U., M.S.K.; Supervision – M.H.U. Resources – M.S.K.; Materials – M.H.U., A.E., S.U., E.E.Ö., A.Ö., K.G., A.Ş., S.S.S., K.Ş., H.E.C., M.A.E., S.A., A.K., M.S.K.; Data Collection and/or Processing – M.H.U., A.E., S.U., E.E.Ö.; Analysis and/or Interpretation – M.H.U., A.E., S.U., E.E.Ö.,

A.Ö., K.G., A.Ş., S.S.S., K.Ş., H.E.C., M.A.E., S.A., A.K., M.S.K.; Literature Search – M.H.U., A.E., S.U., E.E.Ö., A.Ö., K.G., A.Ş., S.S.S., K.Ş., H.E.C., M.A.E., S.A., A.K., M.S.K.; Writing – M.H.U., A.E., S.U., E.E.Ö., A.Ö., K.G., A.Ş., S.S.S., K.Ş., H.E.C., M.A.E., S.A., A.K., M.S.K.; Critical Review – A.K., M.S.K.

**Declaration of Interests:** The authors have no conflicts of interest to declare.

**Funding:** The authors declare that this study received no financial support.

### REFERENCES

- Ratosa I, Ivanetic Pantar M. Cardiotoxicity of mediastinal radiotherapy. *Rep Pract Oncol Radiother.* 2019;24(6):629-643. [CrossRef]
- Díaz-Gavela AA, Figueiras-Graillet L, Luis ÁM, et al. Breast radiotherapy-related cardiotoxicity. When, how, why. Risk prevention and control strategies. *Cancers (Basel).* 2021;13(7):1712. [CrossRef]
- Herrmann J. Adverse cardiac effects of cancer therapies: cardiotoxicity and arrhythmia. *Nat Rev Cardiol.* 2020;17(8):474-502. [CrossRef]
- McMurray JJV, DeMets DL, Inzucchi SE, et al. A trial to evaluate the effect of the sodium-glucose co-transporter 2 inhibitor dapagliflozin on morbidity and mortality in patients with heart failure and reduced left ventricular ejection fraction (DAPA-HF). *Eur J Heart Fail.* 2019;21(5):665-675. [CrossRef]
- Balcioglu AS, Çelik E, Şahin M, Göçer K, Aksu E, Aykan AÇ. Dapagliflozin improves cardiac autonomic function measures in Type 2 diabetic patients with cardiac autonomic neuropathy. *Anatol J Cardiol.* 2022;26(11):832-840. [CrossRef]
- Balcioglu AS, Çelik E, Aksu E, Aykan AÇ. Impact of sodium-glucose Cotransporter-2 inhibitors on sympathetic nervous system activity detected by sympathetic activity index and LF/HF ratio in patients with type 2 diabetes mellitus. *Turk Kardiyol Dern Ars.* 2022;50(6):415-421. [CrossRef]
- Chang WT, Lin YW, Ho CH, Chen ZC, Liu PY, Shih JY. Dapagliflozin suppresses ER stress and protects doxorubicin-induced cardiotoxicity in breast cancer patients. *Arch Toxicol.* 2021;95(2):659-671. [CrossRef]
- Chang WT, Shih JY, Lin YW, et al. Dapagliflozin protects against doxorubicin-induced cardiotoxicity by restoring STAT3. *Arch Toxicol.* 2022;96(7):2021-2032. [CrossRef]
- Avagimyan A, Sheibani M, Pogosova N, et al. Possibilities of dapagliflozin-induced cardioprotection on doxorubicin + cyclophosphamide mode of chemotherapy-induced cardiomyopathy. *Int J Cardiol.* 2023;391:131331. [CrossRef]
- Charan J, Kantharia ND. How to calculate sample size in animal studies? *J Pharmacol Pharmacother.* 2013;4(4):303-306. [CrossRef]
- Boerma M, Sridharan V, Mao XW, et al. Effects of ionizing radiation on the heart. *Mutat Res Rev Mutat Res.* 2016;770(Pt B):319-327. [CrossRef]
- Boerma M, Kruse JJ, van Loenen M, et al. Increased deposition of von Willebrand factor in the rat heart after local ionizing irradiation. *Strahlenther Onkol.* 2004;180(2):109-116. [CrossRef]
- Bakshi MV, Barjaktarovic Z, Azimzadeh O, et al. Long-term effects of acute low-dose ionizing radiation on the neonatal mouse heart: a proteomic study. *Radiat Environ Biophys.* 2013;52(4):451-461. [CrossRef]
- Moro C, Jouan MG, Rakotavoa A, et al. Delayed expression of cytokines after reperfused myocardial infarction: possible trigger for cardiac dysfunction and ventricular remodeling. *Am J Physiol Heart Circ Physiol.* 2007;293(5):H3014-H3019. [CrossRef]

15. Chen K, Keaney JF Jr. Evolving concepts of oxidative stress and reactive oxygen species in cardiovascular disease. *Curr Atheroscler Rep.* 2012;14(5):476-483. [\[CrossRef\]](#)
16. Cilliers GD, Harper IS, Lochner A. Radiation-induced changes in the ultrastructure and mechanical function of the rat heart. *Radiother Oncol.* 1989;16(4):311-326. [\[CrossRef\]](#)
17. Walls GM, O'Kane R, Ghita M, et al. Murine models of radiation cardiotoxicity: a systematic review and recommendations for future studies. *Radiother Oncol.* 2022;173:19-31. [\[CrossRef\]](#)
18. Gürses I, Özeren M, Serin M, Yücel N, Erkal HŞ. Histopathological evaluation of melatonin as a protective agent in heart injury induced by radiation in a rat model. *Pathol Res Pract.* 2014;210(12):863-871. [\[CrossRef\]](#)
19. Wang K, Eblan MJ, Deal AM, et al. Cardiac toxicity after radiotherapy for Stage III non-small-cell lung cancer: pooled analysis of dose-escalation trials delivering 70 to 90 Gy. *J Clin Oncol.* 2017;35(13):1387-1394. [\[CrossRef\]](#)
20. Bradley JD, Paulus R, Komaki R, et al. Standard-dose versus high-dose conformal radiotherapy with concurrent and consolidation carboplatin plus paclitaxel with or without cetuximab for patients with stage IIIA or IIIB non-small-cell lung cancer (RTOG 0617): a randomised, two-by-two factorial phase 3 study. *Lancet Oncol.* 2015;16(2):187-199. [\[CrossRef\]](#)
21. Kovács MG, Kovács ZZA, Varga Z, et al. Investigation of the antihypertrophic and antifibrotic effects of losartan in a rat model of radiation-induced heart disease. *Int J Mol Sci.* 2021;22(23):12963. [\[CrossRef\]](#)
22. Schlaak RA, Frei A, Fish BL, et al. Acquired immunity is not essential for radiation-induced heart dysfunction but exerts a complex impact on injury. *Cancers (Basel).* 2020;12(4):983. [\[CrossRef\]](#)
23. Ellahham S, Khalouf A, Elkhazendar M, Dababo N, Manla Y. An overview of radiation-induced heart disease. *Radiat Oncol J.* 2022;40(2):89-102. [\[CrossRef\]](#)
24. Curtain JP, Docherty KF, Jhund PS, et al. Effect of dapagliflozin on ventricular arrhythmias, resuscitated cardiac arrest, or sudden death in DAPA-HF. *Eur Heart J.* 2021;42(36):3727-3738. [\[CrossRef\]](#)
25. Fernandes GC, Fernandes A, Cardoso R, et al. Association of SGLT2 inhibitors with arrhythmias and sudden cardiac death in patients with type 2 diabetes or heart failure: a meta-analysis of 34 randomized controlled trials. *Heart Rhythm.* 2021;18(7):1098-1105. [\[CrossRef\]](#)
26. Saiki H, Moulay G, Guenzel AJ, et al. Experimental cardiac radiation exposure induces ventricular diastolic dysfunction with preserved ejection fraction. *Am J Physiol Heart Circ Physiol.* 2017;313(2):H392-H407. [\[CrossRef\]](#)
27. Lancellotti P, Nkomo VT, Badano LP, et al. Expert consensus for multi-modality imaging evaluation of cardiovascular complications of radiotherapy in adults: a report from the European Association of Cardiovascular Imaging and the American Society of Echocardiography. [published correction appears in *Eur Heart J Cardiovasc Imaging.* 2013;14(12):1217. [\[CrossRef\]](#)]. *Eur Heart J Cardiovasc Imaging.* 2013;14(8):721-740. (<https://doi.org/10.1093/ehjci/jet123>)
28. Cuomo JR, Sharma GK, Conger PD, Weintraub NL. Novel concepts in radiation-induced cardiovascular disease. *World J Cardiol.* 2016;8(9):504-519. [\[CrossRef\]](#)
29. Ma CX, Zhao XK, Li YD. New therapeutic insights into radiation-induced myocardial fibrosis. *Ther Adv Chronic Dis.* 2019;10:2040622319868383. [\[CrossRef\]](#)